Received: 20 January 2020 | Accepted: 4 February 2020

DOI: 10.1002/maco.202011540

ARTICLE

Materials and Corrosion

SMART-DECK: Multifunctional carbon-reinforced concrete interlayer for bridges

Carla Driessen-Ohlenforst

Dedicated to Professor Dr.-Ing. Michael Raupach on the occasion of his 60th birthday

Institute of Building Materials Research, RWTH University, Aachen, Germany

Correspondence
Carla Driessen-Ohlenforst, Institute of Building Materials Research, RWTH University, Schinkelstr. 3, 52062 Aachen, Germany.
Email: driessen@ibac.rwth-aachen.de

Funding information
Bundesministerium für Bildung und Forschung

Abstract

The service life of bridges is often threatened by an insufficient shear force capacity in the transverse direction as well as by leakages in the sealing layer, which leads to chloride ingress and therefore corrosion damages. To prevent expensive repair work and traffic obstructions, a thin, multifunctional interlayer of textile-reinforced concrete called SMART-DECK was developed. This interlayer provides three functions: A full-surface moisture monitoring in real-time, a preventive cathodic corrosion protection, and an increase of the shear force capacity. The operator of the bridge is able to monitor the condition of the sealer in real-time. The relevant data are transmitted via the internet and show the condition of the sealer in a simple color scheme. If leakage occurs, the cathodic corrosion protection can be switched on to protect the reinforcement from corrosion damages. The renewing of the damaged bridge deck sealing has not to be carried out immediately but can be postponed over years, for example, to periods with little traffic. In this paper, the scientific approach for the realization of the system is presented, beginning with laboratory pretests on the materials and numerical simulations. The results are used to test the functions of the system in the laboratory and later on two demonstrators. An outlook will present the next research questions.

KEYWORDS

carbon, cathodic prevention, monitoring, resistivity measurements, textile-reinforced concrete

1 | INTRODUCTION

A sustainable and efficient transport infrastructure becomes more and more important because of the increasing traffic density. Damages on bridges lead to reduced service life and to long-term problems: Chloride ions can migrate into the concrete, which causes corrosion of the reinforcement and thus threatens the durability of the construction. The corrosion of the reinforcement can only be seen on the surface of the bridge when a high degree of impairment is already reached. At that point, comprehensive building operations are necessary, which leads to traffic obstructions and thus to economic losses. By now, sensors for the monitoring of humidity in constructions or sensors, which help to

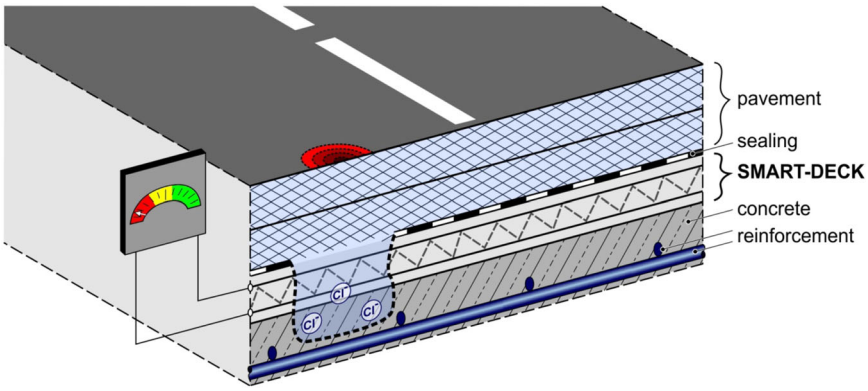

FIGURE 1 Schematic representation of the structure and functioning of SMART-DECK [Color figure can be viewed at wileyonlinelibrary.com]

estimate the probability of corrosion exist, but these sensors work only discretely at the point of installation.[1] The monitoring of a complete construction would need a high number of sensors, which often is not economic. The interlayer will be divided into sections, which are arranged transverse to the lane. Each section builds a separate sensor. Two technical textile layers are arranged with a spacing of 15 mm. The electrical resistivity between the two layers is measured as seen in Figure 1. When the sealing starts to leak and water permeates into the interlayer, a drop in the measured electrical resistivity is detected and the operator of the bridge construction receives a note about the leakage. It is planned to monitor the condition of the sealing in real-time. Therefore, all relevant data are transmitted via the internet and are presented in a simple form, for example, in a color scheme. When an event of damage in the sealing is detected, the cathodic corrosion protection can be switched on. Thus, the constructional measures of the bridge deck sealing can be postponed to periods with less traffic or to that point of time when a renewing of the sealing is planned anyway. With a rectifier, an electrical field is generated between the carbon and the reinforcement, which disables chloride migration into the construction. Thus, the depassivation of steel is prevented.[2]

2 | STRUCTURE AND MATERIALS

SMART-DECK is constructed modularly, meaning that the three functions can be installed in various combinations needed for the particular building. For example, if the load-bearing capacity of the bridge is sufficient, only the monitoring and the function of the preventive cathodic protection will be installed. In this case, the system can be reduced by one carbon layer and becomes even thinner reducing the carbon needed and costs. The modularity allows the installation of the system in existing constructions as well as in new bridges. The general structure consists of two carbon meshes, which are kept at a distance of 15 mm with spacers and placed on the shot-blasted construction concrete. The covering of the mortar above and below the carbon meshes is 10 mm. The interlayer covers the full-bridge superstructure between the cantilevers. At the moment the average measuring field has a width of 1.20 m. The length depends on the width of the bridge. The measuring fields have a spacing of 20 mm between each other to guarantee electrical disconnection.

2.1 | Textile carbon reinforcement

The reinforcement of SMART-DECK is biaxial carbon meshes with a mesh size of 38 mm. These are impregnated with a special epoxy resin. To guarantee the spacing between the carbon meshes and the spacing to the construction concrete, insulating spacers are preinstalled. To prevent floating of the carbon reinforcement during the pouring of the mortar the carbon meshes are anchored. Figure 2 shows the carbon meshes with the spacers before the pouring of the mortar.

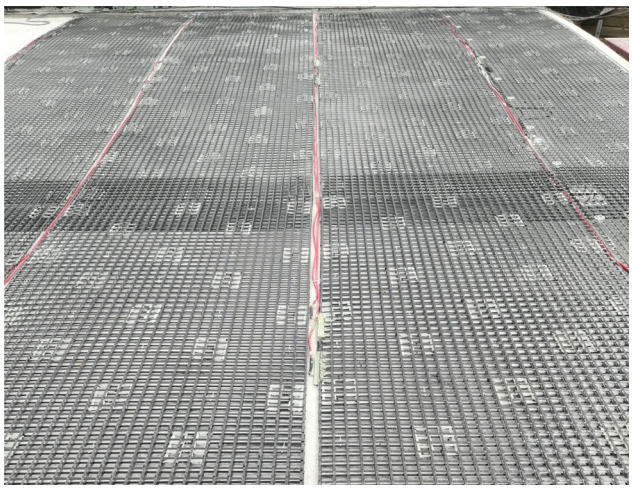

FIGURE 2 Carbon textile reinforcement of some measuring fields before placement of the mortar [Color figure can be viewed at wileyonlinelibrary.com]

2.2 | Mortar

A high-performance mortar, specially developed for the project was used. The mortar has a maximum grain size of 4 mm. It meets the competing demands of being flowable enough that the textile reinforcement is fully embedded and being stable enough to enable the manufacturing of a gradient of 2.5% of inclination of the road.

To receive a finely graduated humidity-monitoring it is necessary that the mortar has a high sensitivity for humidity, which means that the mortar should have a wide range in resistivity values at different moisture contents. To reach this objective, a suitable pore structure has to be found. In this context, capillary pores with low constrictivity and tortuosity could achieve the intended properties.[3] Therefore, a screening of different mortars was conducted by investigating the water content/resistivity behavior of the mortars.[4] The procedure is described in the next chapter.

3 | MONITORING

3.1 | Relationship between water content and resistivity

The detection of leakages is based on a measurement of the resistance between two layers of carbon textile. Using calibration curves one can conclude the water content of the mortar from the resistivity values.[5] Under an intact sealer after a few years of dessication the mortar shows high resistivity values. If leakage occurs, water permeates into the interlayer and a drop in resistance is measured. Empirically, a frequency of 108 Hz provides good results. At this frequency, no significant polarization of the electrodes occurs and this frequency guarantees that the cable length does not lead to a falsification of the measured values. For SMART-DECK, a voltage of 2 V was chosen. Impedance tests showed that 108 Hz lays in the acceptable frequency range. Figure 3 shows the impedance and phase angle for a frequency range from 10 to 10,000 Hz for the SMART-DECK set up for two different time points.

The calibration curves for the relation between water content and resistivity were prepared in the laboratory using a two-electrode setup. An alternating voltage is applied and the resulting current is measured. The ratio of these values leads to the alternating current resistance, respectively the electrolyte resistance of the mortar. Using Ohm's law:

$$R = U/I, \tag{1}$$

where R is the electrolyte resistance (Ω), U is the applied voltage (V), and I is the current (A).

For the investigations, frequencies from 100 Hz to 100 kHz are tested. The resistances depend on the geometry of the specimen. To compensate this, a geometry factor is used.

$$\rho = R \cdot k, \tag{2}$$

where ρ is the resistivity (Ω·m), R is the electrolyte resistance (Ω), and k is the geometry factor (m).

For these measurements, the specimens are stored underwater until the measured resistivity values stay constant. The measured values and the weight of the specimens are recorded. Afterward, the specimens are dried to reach low water contents. Starting at these contents, different moisture contents are being adjusted

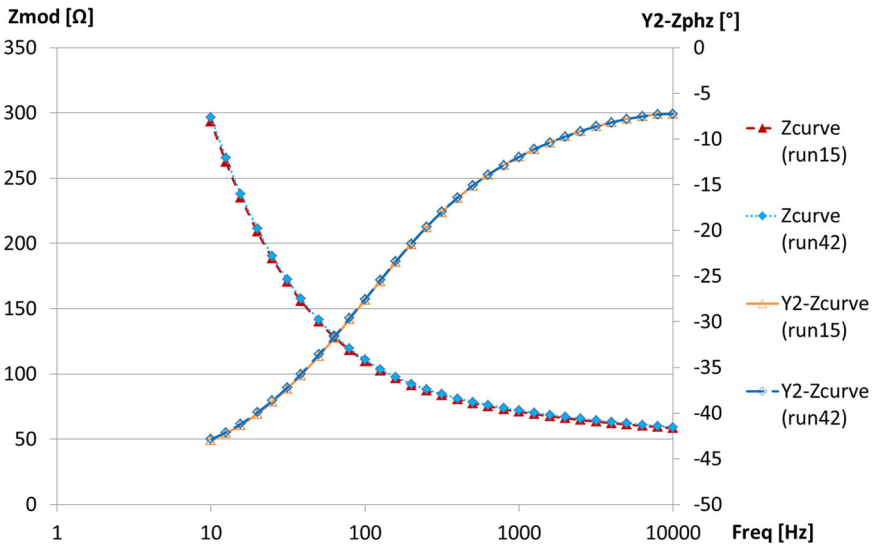

FIGURE 3 Impedance and phase angle for 10–10,000 Hz [Color figure can be viewed at wileyonlinelibrary.com]

through the addition of different amounts of water. The specimens are being packed in a closed environment to reach a homogenous distribution of the water. After 2 weeks, the specimens are being unpacked and weighed. The resistivity is being measured before the specimens are dried again up to a constant weight and are then weighed again. Based on these data the relationship between humidity and resistivity values can be calculated.

Having determined the resistivity values with the corresponding moisture contents, a regression analysis is carried out using the following regression function[6,7]:

$$u = \frac{A}{\ln(B \cdot \rho + C) - D} + E, \tag{3}$$

where u is the moisture content in M% referred to the mass of mortar, ρ is mortar resistivity (Ω·m), and A and E are regression parameters.

The measured values and the respective regression curve can be seen in Figure 4 for the chosen mortar (M2). As a reference, two other mortars (M1 and M3), which were tested are pictured. However, mortar M3 showed a more disadvantageous rheological behavior than mortar M2. For mortar M1, one can see that the regression curve evolves with a lower gradient and therefore shows a lower sensitivity. Hence, mortar M2 was chosen and is the base for all subsequent investigations.

3.2 | Numerical simulations

Using the calibration curve as an input parameter, numerical simulations were carried out. As the main question it should be investigated, which leakage size of the sealer is detectable under different boundary conditions such as the resistivity values of the dry mortar under an intact sealer or the soaked mortar in a leakage zone. Other influencing parameters are the position of the leakage in the measuring field and the form of the leakage or the depth up to which water is soaked into the mortar. Based on the laboratory tests, resistivity values up to 1,000 Ω·m represent a soaked mortar in a leakage zone and resistivity values above 1,000 Ω·m correspond to a dry mortar under the intact sealer. However, these values cannot be interpreted as a sharp threshold. The greater the difference in resistivity values between a dry and a soaked mortar the easier becomes the detection of leakages. Furthermore, detection becomes easier with greater leakage sizes and smaller measuring fields. The numerical simulations showed that even leakages of a few percentages of the total field size are detectable. The other main result is that besides the resistivity values and the leakage size only the depth of a leakage shows a significant influence on the detectability.[8]

3.2.1 | Comparison between one and two carbon layers

Simulations were carried out for two different variants of SMART-DECK.

- For the standard setup where the resistance is measured between the two carbon meshes.
- For the possible setup with just one carbon layer where the resistance is measured between the carbon layer and the steel reinforcement of the construction concrete.

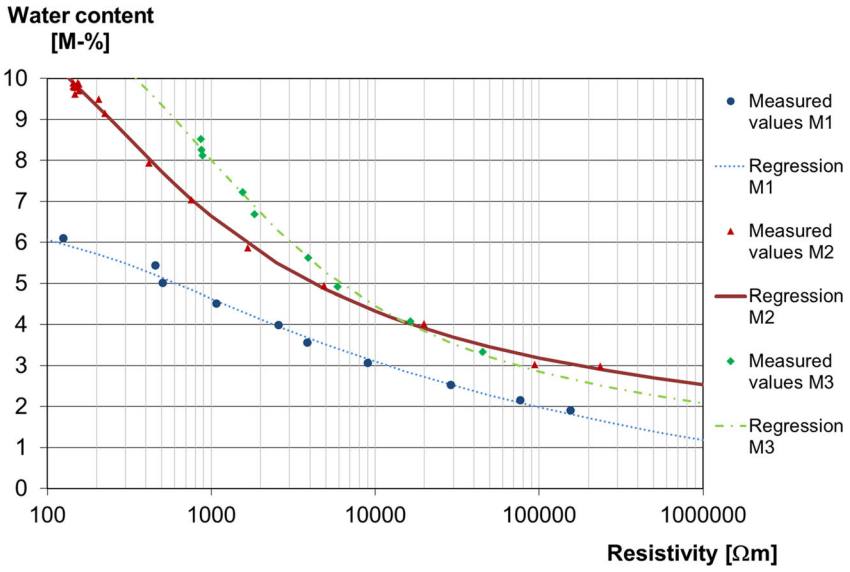

FIGURE 4 Relationship between water content and resistivity of the investigated mortars [Color figure can be viewed at wileyonlinelibrary.com]

For the second option, the resistivity values of the construction concrete were presumed to be three times higher than the respective presumed resistivity values of the SMART-DECK mortar, because it is expectable that the construction concrete dried up over decades before the first damage of the sealing occurs. For these simulations, the AC–DC module of the software COMSOL Multiphysics was used. For the electrical potential of an electrolyte in an electrical field, the following equation holds in general[9]:

$$-\nabla(\varepsilon_0 \times \varepsilon_r \times \nabla V) = 0, \tag{4}$$

where V is the potential (V), $\boldsymbol{\varepsilon_0}$ is the electrical field constant, and ε_r is the relative permittivity.

With the assumption of an isotropic material of the electrolyte, a constant frequency and temperature as well as a constant magnetic and electrical external field, Equation (4) can be rewritten as[10]:

$$\Delta V = 0. \tag{5}$$

So the potential in the mortar can be computed under the mentioned assumptions for given boundary conditions, that is, potentials or voltages of the carbon layers, respectively.

The relationship between potential, current density, and electrolyte resistance is described by Ohm's law, which can be expressed with the following formula assuming isotropic electrolytes[11]:

$$i = -\frac{1}{\rho}\nabla V, \tag{6}$$

where i is the current density (A/m^2), ρ is the resistivity (Ω·m), and V is the potential (V).

The differential equation system consisting of Equations (5) and (6) is solved numerically with Comsol to compute the resistivity ρ as an output parameter.

In this context, the voltage applied can be chosen arbitrarily because it will be offset by the resulting current (cf. Equation 6).

Figure 5 compares the simulated resistivity drops for intruding water for the standard structure on the left side and the structure with the measuring field between one carbon layer and the reinforcement on the right. The resistivity drops caused by leakage and intruding water

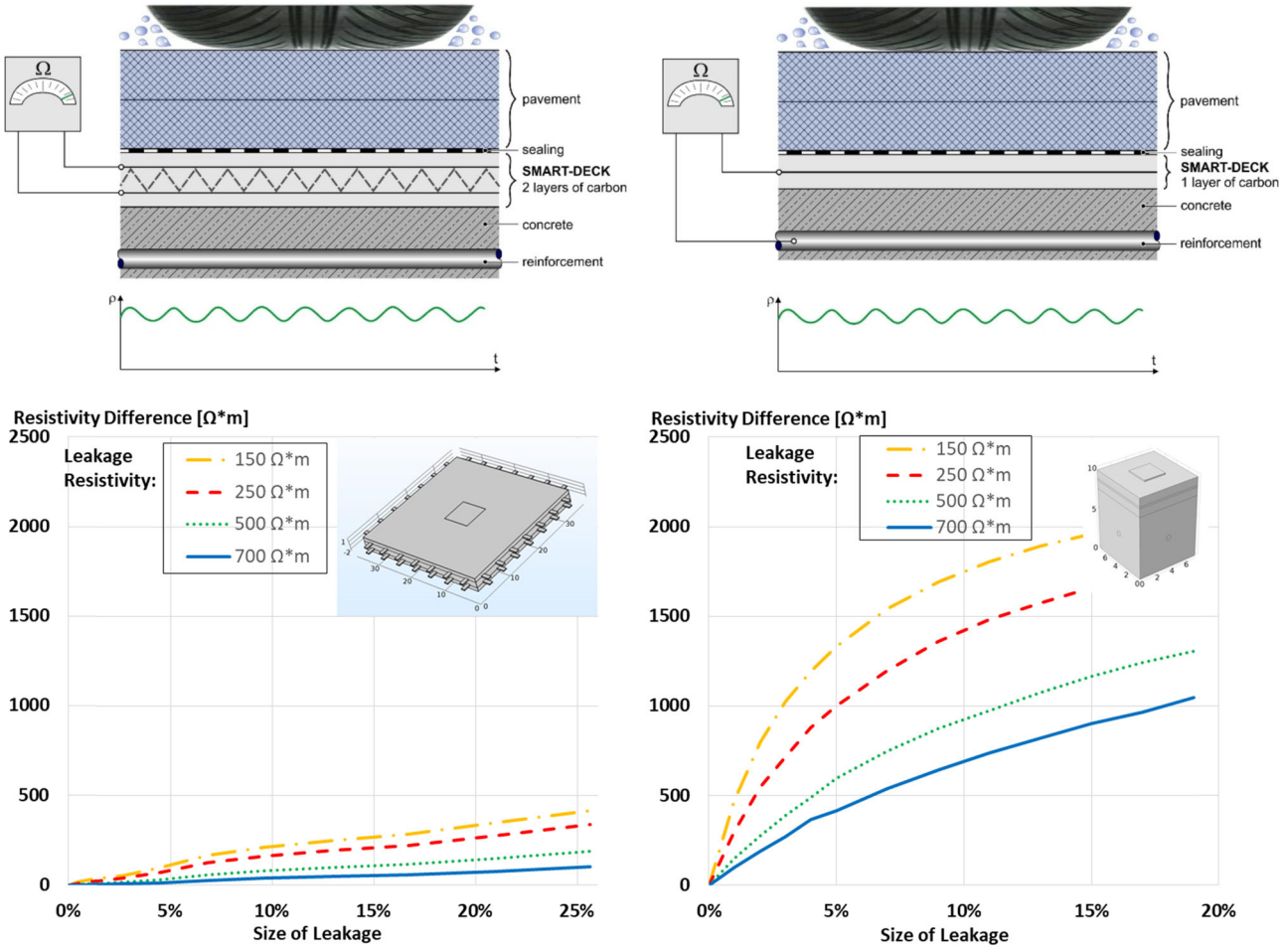

FIGURE 5 Simulated resistivity drops for different structures, different leakage sizes, and various initial resistivities [Color figure can be viewed at wileyonlinelibrary.com]

are greater for the version on the right side due to the greater resistivity value of the construction concrete and therefore the greater difference to the values of the soaked mortar in the leakage zone. With a measuring resolution up to 0.01 Ω·m, leakages of a few percentages of the total field size are detectable for both versions. Nevertheless, one has to take into account that the original structure with two carbon meshes allows the detection of leakages in the SMART-DECK layer while in the second version the chloride-contaminated water has already reached the construction concrete when detection is possible. Of course, the resistivity values decrease with the depth of the leakage. The simulated resistivity values over the depth of the measuring field are compared in Figure 6. In this example, a mortar resistivity of 1,000 Ω·m and a concrete resistivity of 3,000 Ω·m were presumed. This leads to a combined resistivity of approximately 2,630 Ω·m as a reference resistivity in a condition without leakages for the version with one carbon layer. Starting from this reference resistivity a clear drop in the resistivity values for this version can be seen at first at a depth between 3 and 4 cm, thus in the area of the construction concrete. So, one has to weigh between the advantages of the one-carbon layer version, which are the reduced costs and the thinner layer thickness, and the disadvantages like the deeper chloride ingress. Furthermore, different possible reinforcement ratios and construction concrete lead to more varying conditions in the SMART-DECK version with just one carbon layer, which makes further investigations necessary.

3.3 | Monitoring in laboratory tests

To test the detectability of leakages, in the laboratory artificial leakages were produced on the top of mortar specimens. Specimens with a size of $440 \times 480 \times 35\ mm^3$ were cast. The structure with two carbon meshes with a spacing of 15 mm was used. The specimens were sealed with epoxy by leaving out artificial leakages. On each specimen, a different form, size, or position of the leakage was tested. To guarantee a permanent water admission, water basins were formed on top of the specimen, as illustrated in Figure 7. The carbon meshes of the specimens have electrical connections for a continuous resistance measurement during the testing time. The resistance is measured with frequencies between 10 Hz and 10 kHz. Figure 8 shows an exemplary plot of resistance measurement. For 2 days, the resistance was measured before water was applied. The resistance measurement was pursued without a break during the water admission, so one

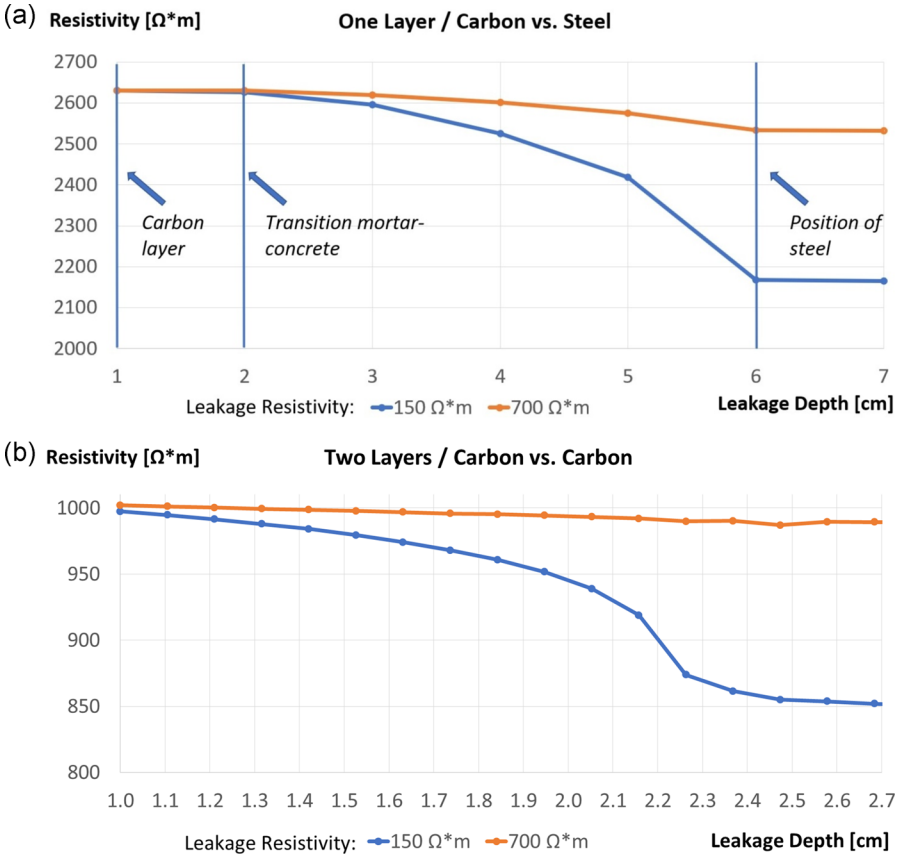

FIGURE 6 (a) Resistivity values as a function of the leakage depth for the one-textile-layer version. (b) Resistivity values as a function of the leakage depth for the two-textile-layer version [Color figure can be viewed at wileyonlinelibrary.com]

FIGURE 7 Specimen for the detectability-test with two artificial leakages [Color figure can be viewed at wileyonlinelibrary.com]

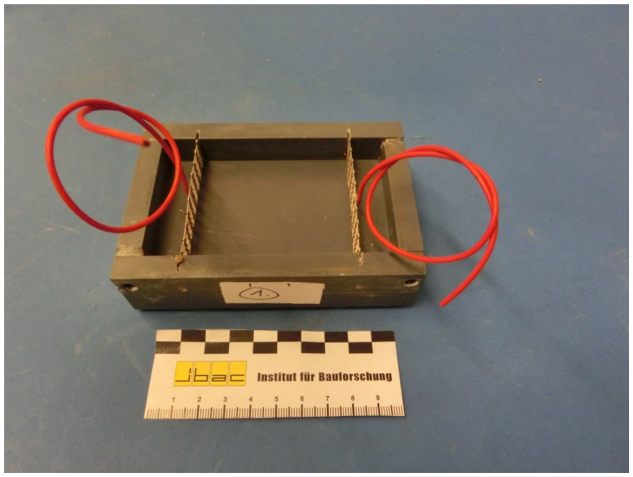

FIGURE 9 Specimen for the investigation of the temperature dependence of the mortar [Color figure can be viewed at wileyonlinelibrary.com]

can see that a few hours after water admission a significant drop in resistance at all frequencies occurs. The discrepancy of the 10 Hz curve can be explained by a polarization of the electrodes at this frequency.

Besides the moisture content, the temperature has a great impact on the resistance. With increasing temperatures in the structure, the ion mobility within the electrolyte increases and the conductivity increases as well.[12] The impact of temperature in concrete can be described by the Arrhenius equation.[13]

$$R_1 = R_0 \times e^{b*\left(\frac{1}{T_1}-\frac{1}{T_0}\right)}, \quad (7)$$

where R_0 is the electrolyte resistance (Ω) at the temperature T_0, R_1 is the measured electrolyte resistance (Ω) at the temperature T_1, and b is the temperature coefficient (K).

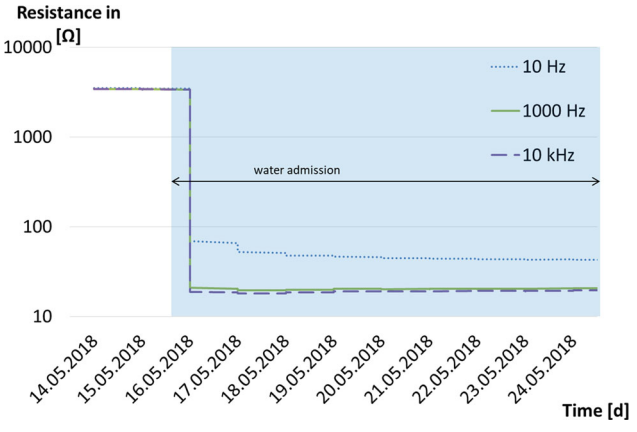

FIGURE 8 Exemplary resistance measurement during water admission [Color figure can be viewed at wileyonlinelibrary.com]

The temperature coefficient should be determined for each mortar or concrete. In the literature, a range between 3,000–7,000 K is mentioned depending on the moisture content and concrete properties, see for example [13–15]. For a temperature compensation of the resistance values, the temperature coefficient for the SMART-DECK mortar was investigated in the laboratory. Therefore, the specimens with a two-electrode set up inside, which are pictured during preparation in Figure 9, were partially saturated (25–30%; 60–65%; 85–100% moisture content). After the adjustment of the water content the specimen was sealed with epoxy and stored under different temperatures (−10°C, −2°C, 0°C, 5°C, 20°C, and 50°C). For the SMART-DECK mortar, a temperature coefficient of 4,040 K for the estimated initial saturation of the mortar could be validated as appropriate, which can be seen in Figure 10. As the temperature coefficient depends on the humidity with the ongoing desiccation of the mortar the appropriate coefficient will change.

3.4 | Monitoring on outdoor demonstrators

Besides the investigations in the laboratory, two outdoor demonstrators were built. The first has a size of 80 m². The aim was to test the detectability of leakages under real weather conditions. On the demonstrator four electrically disconnected measuring fields were realized. The electrical connections were made and cables stored in a control box near the demonstrator. As in the laboratory, artificial leakages were produced by applying water basins on the surface of the demonstrator and sealing the rest of the surface with epoxy. Water basins were used to

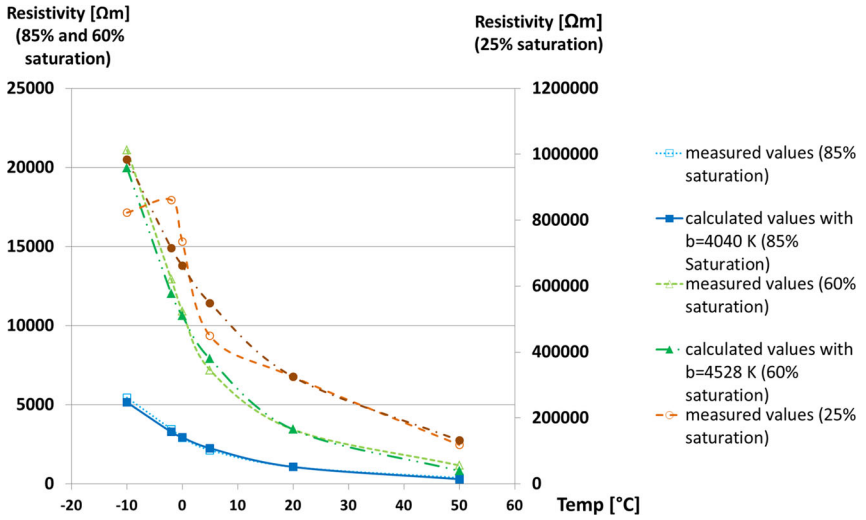

FIGURE 10 Validation of the temperature compensation [Color figure can be viewed at wileyonlinelibrary.com]

prevent fast desiccation because it is assumed that if real leakages occur in the sealing layer an accumulation of water over the SMART-DECK layer takes place. Figure 11 shows the surface with the artificial leakages. Again different forms, sizes, and positions of the leakages were tested. The newly developed full-surface resistance measurement is simultaneously verified via multiring sensors. These sensors normally have nine rings of stainless steel separated by isolated plastic rings. By applying an alternating voltage the resistance between neighboring rings can be measured. That way one receives a graded profile of the resistance over the depth.[7,16,17] However, the comparison of these two measuring techniques can only give an estimation of the correctness of the values. The resistance can be measured with a resolution of 0.01 Ω up to values of 20 Ω and with a resolution of 0.1 Ω over this value. Figure 12 shows a part of the data transmission of the measuring values of the demonstrator. Recorded are the resistance values, the temperature, and the temperature-compensated resistance values. It can be seen that the resistance values follow the temperature fluctuations over the day, which shows a good sensitivity of the measuring technique. Furthermore, this ensures that no short circuits between the two carbon layers exist, which could be the case when during the mortar pouring the two carbon layers are pressed together. During the few test months of the demonstrator only a slow increase in the resistivity values could be observed showing the desiccation of the plate. Due to the high water content of the fresh mortar a leakage detection was not yet possible.

Therefore, a second demonstrator on a newly constructed bridge was realized in 2019. The resistivity values will be measured over years and the measuring technique will be tested for the first time under real traffic conditions. The second modification in comparison with the first demonstrator is the power supply, which will be ensured with a solar panel placed near the bridge construction. So even on bridges where no electricity grid is available SMART-DECK can be applied. The cables from the carbon layers are led over a short distance to the solar panel and a measuring box. On the pole of the solar panel

FIGURE 11 Sealed demonstrator with artificial leakages [Color figure can be viewed at wileyonlinelibrary.com]

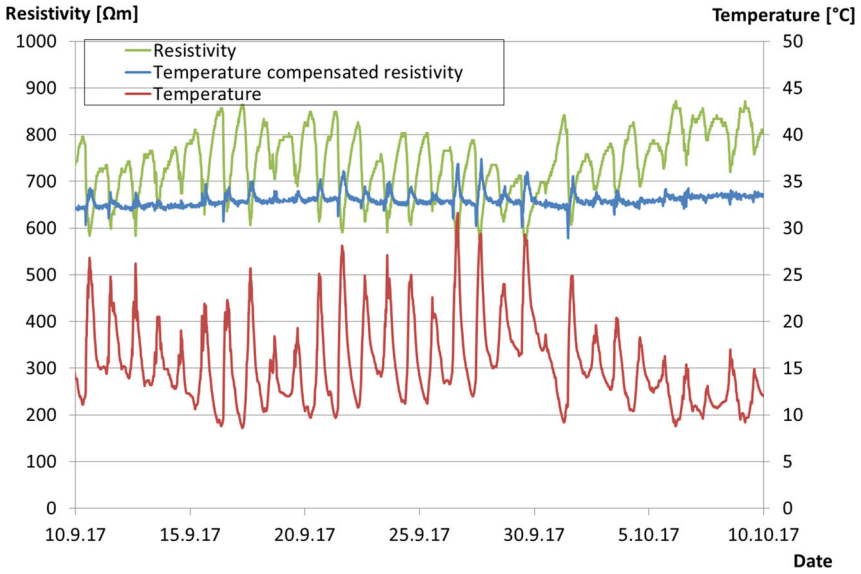

FIGURE 12 Temperature, resistivity, and temperature-compensated resistivity of one measuring field [Color figure can be viewed at wileyonlinelibrary.com]

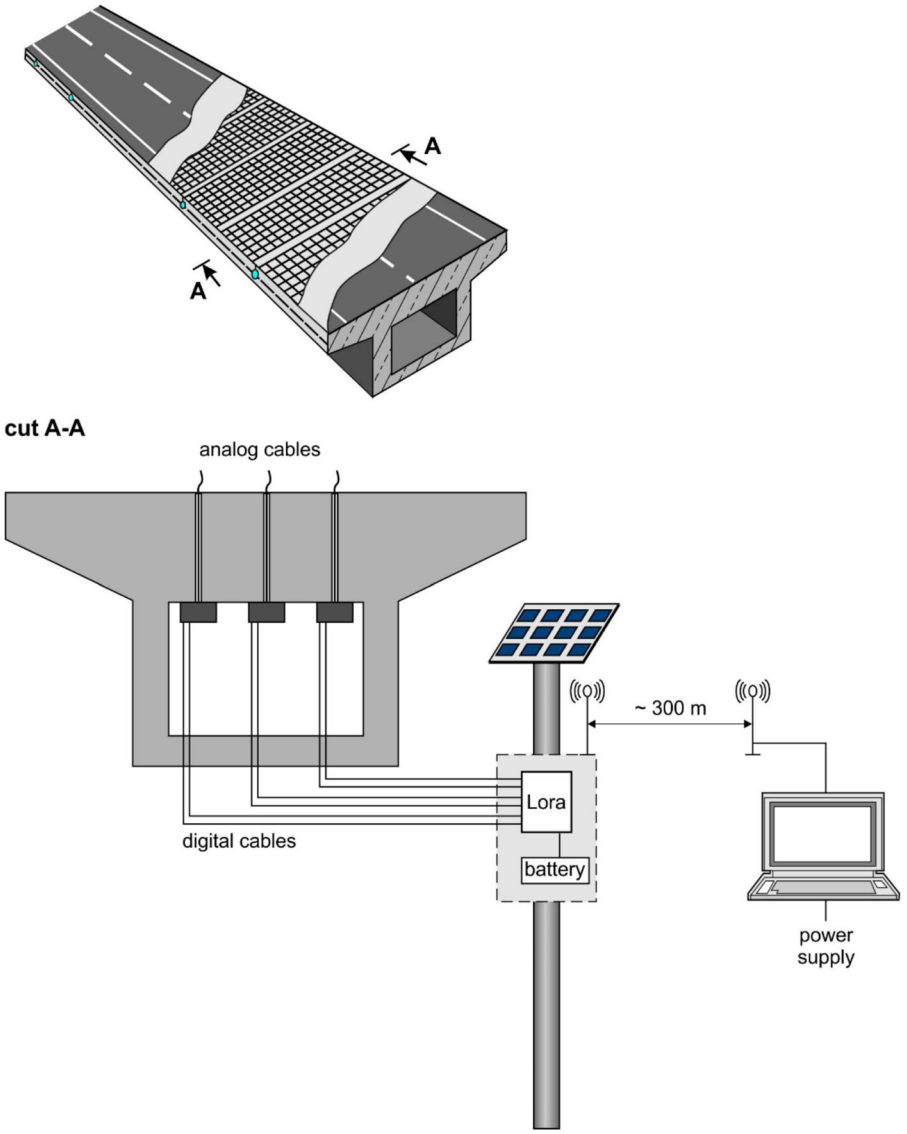

FIGURE 13 Data transmission [Color figure can be viewed at wileyonlinelibrary.com]

a module is attached, which provides the measuring data from the bridge via LoRa-technique (long-range wide area network) to a computer, which is placed in a nearby building. From there the data can be accessed via a remote connection, see Figure 13.

As in the first demonstrator temperature sensors as well as multiring sensors were installed. Until now, the measuring technique, the solar power supply, and the data transmission with LoRa have been tested on the university ground and will be started at the demonstrator bridge in the next weeks.

4 | FURTHER FUNCTIONS OF SMART-DECK

4.1 | Cathodic prevention

If the monitoring data show a leakage in the bridge deck sealing, which cannot be repaired immediately, the cathodic prevention is switched on. In this case, the carbon layers serve as an impressed current anode. The prevention of chloride-induced corrosion of steel in concrete through impressed current is nowadays established (see for example [18–20]). The suitability of carbon textiles as an impressed current anode has been investigated, for example, by Asgharzadeh.[21] Potentiostatic tests showed that carbon textiles deliver a constant current over the investigation period and a cathodic protection with carbon textiles is possible without a destruction of the carbon as long as a polarization of the anode of more than 2,200 mV vs normal hydrogen electrode is excluded.

While cathodic protection is used for structures already affected by chloride-induced corrosion, cathodic prevention is used for structures that will presumably be contaminated by chlorides.[22] Cathodic prevention relies on the fact that the critical chloride threshold increases as the potential of steel decreases. So even very low current densities ($<2\,mA/m^2$) polarize the reinforcement to values, in which steel works under conditions of "imperfect passivity" so that initiation of pitting is prevented even if high levels of chlorides accumulate at the surface of the steel by penetrating through the cover concrete.[22,23]

On the first outdoor demonstrator the cathodic prevention was tested in realizing different protection zones with different reinforcement ratios. In accordance with Reference [14] the effect of the cathodic prevention was tested in carrying out a depolarization measurement. The anodic potential shift after a 24-hr disconnection of the power supply was higher than 150 mV, which indicates that the carbon textiles embedded in the selected mortar are a suitable anode system. The first and second outdoor demonstrator of SMART-DECK are one of the first large-scale testing areas for cathodic protection systems with carbon reinforcement. By now, the functionality of carbon as an impressed current anode in concrete was only tested on small specimens as in Reference [21].

4.2 | Strengthening

The third function was investigated at the Institute for Structural Concrete of the RWTH Aachen University. The strengthening effect was examined with regard to its flexural and shear capacity. With tests on small-scale specimens, the load-bearing properties of different combinations of the textiles and mortar were investigated. Therefore, reinforced concrete slab segments were strengthened with a carbon-reinforced concrete layer. For investigating the bending and shear capacity, the load position and the tensile reinforcement ratio were varied. The influence of the additional layer on crack formation and capacity was examined. The investigations showed that a strengthening of bridge deck slabs with SMART-DECK is possible.[24] Regarding the bending strength, a duplication of the bearing capacity was achieved and concerning the shear force capacity an increase of 23.5% and 56% was reached.[25]

5 | CONCLUSION AND OUTLOOK

The described investigations and results can be summarized as follows:

- The numerical simulations showed that leakages of a few percentages of the total field size are detectable with the single-layer setup or the standard structure of SMART-DECK.
- Laboratory tests proved the simulated detectability of artificial leakages through resistance measurement
- The measuring technique and data transmission was tested on the first demonstrator and installed under real traffic conditions on a real bridge construction

In the next months SMART-DECK will be tested under real traffic conditions and with an alternative power supply.

On the scientific side the question, "which potential gradients are necessary to prevent chloride ions from migrating into the matured concrete and from damaging the reinforcing steel" is investigated. By applying an electrical field between the carbon meshes and the steel, the negatively charged chloride ions will be held on the carbon mesh, which is polarized as an anode. It could be possible that the resulting current densities are smaller than they have to be for the common (preventive) cathodic protection,

so that an electrochemical chloride barrier is implemented. Therefore, laboratory test as well as numerical simulations were carried out in materials with different diffusion resistances and with different potential gradients. The results will be presented in publications in the next months.

ACKNOWLEDGMENTS

The authors would like to thank the BMBF for funding the project and the project executing organization, "VDI Technologiezentrum GmbH (VDI TZ)" for the support. The project partners are: Bundesanstalt für Straßenwesen (BASt), Eurovia Beton GmbH NL Bauwerksinstandsetzung (project coordination), Solidian GmbH (Albstadt-30 Lautlingen), Massenberg GmbH, instakorr GmbH (Darmstadt), Sto Cretec GmbH, Tochtergesellschaft der Sto SE & Co. KGaA and the Institute of Structural Concrete, RWTH Aachen University. Special thanks to the city of Mönchengladbach for the cooperation in building the large-scale demonstrator.

ORCID

Carla Driessen-Ohlenforst http://orcid.org/0000-0002-7023-0931

REFERENCES

[1] M. Raupach, J. Gulikers, K. Reichling, *Mater. Corros.* **2013**, *64*, 141.
[2] M. Raupach, C. Driessen, presented at *ICCRRR*, Leipzig, Germany, October **2015**, pp. 537-540.
[3] K. Reichling, O. Weichold, M. Raupach, *Restor. Build. Monuments* **2012**, *18*, 265.
[4] C. Driessen, M. Raupach, presented at *Proc. Eighth Int. Conf. Bridge Maintenance, Safety and Management*, (IABMAS), Foz do Iguacu, Brazil, June **2016**, pp. 2-3.
[5] W. Elkey, E. J. Sellevold, *Electrical Resistivity of Concrete*, Norwegian Road Research Laboratory, Oslo, Norway **1995**.
[6] J. Harnisch, *Thesis*, RWTH Aachen University (Germany) **2003**.
[7] W. Brameshuber, M. Raupach, P. Schröder, C. Dauberschmidt, presented at *Int. Symp. Non-Destructive Testing in Civil Engineering (NDT-CE)*, Berlin, Germany, September **2003**, Poster No. 41.
[8] C. Driessen, M. Raupach, Selected Papers of the 8th International RILEM Ph.D. Workshop, Marne-la-Vallee, France, September, Springer, Cham, Switzerland **2019**.
[9] U. Krey, A. Owen, *Basic Theoretical Physics. A Concise Overview*, Springer, Berlin, Germany **2007**.
[10] G. Lehner, *Elektromagnetische Feldtheorie für Ingenieure und Physiker*, Springer, Berlin, Germany **2006**.
[11] J. D. Jackson, *Classical Electrodynamics*, John Wiley & Sons, Berlin, Germany **2006**.
[12] K. Osterminski, R. B. Polder, P. Schießl, *Heron* **2012**, *57*, 211.
[13] M. Raupach, C. Dauberschmidt, J. Warkus, presented at Innovative Feuchtemessung in Forschung und Praxis, *Bauwesen-Geotechnik-Umwelttechnik, Kolloquium mit Workshop*, Karlsruhe, Germany, July **2003**, p. 2.
[14] M. Raupach, *Ph.D. Thesis*, RWTH Aachen (Germany) **1992**.
[15] D. Bürchler, *Ph.D. Thesis*, Technische Hochschule Zürich (Switzerland) **1996**.
[16] M. Raupach, C. Dauberschmidt, L. Wolff, J. Harnisch, *Beton* **2007**, *57*, 20.
[17] M. Raupach, C. Dauberschmidt, L. Wolff, presented at *Concrete Repair, Rehabilitation and Retrofitting Concrete Repair*, Cape Town, South Africa, November **2005**, p. 438.
[18] DIN EN ISO 12696: Kathodischer Korrosionsschutz von Stahl in Beton (ISO 12696: **2016**).
[19] T. Eichler, S. Gieler-Breßmer, *Betonkalender, 2019, Parkbauten, Geotechnik und Eurocode 7*, John Wiley & Sons, Berlin, Germany **2019**, pp. 863-904.
[20] B. Isecke, in *Handbook of Cathodic Corrosion Protection*, Gulf Publishing Company, Houston 1997, Ch. 19.
[21] A. Asgharzadeh, *Ph.D. Thesis*, RWTH Aachen (Germany) **2019**.
[22] L. Bertolini, B. Elsener, P. Pedeferri, E. Redaelli, R. Polder, *Corrosion of Steel in Concrete: Prevention, Diagnosis, Repair*, Wiley-VCH Verlag, Weinheim, Germany **2013**.
[23] L. Bertolini, F. Bolzoni, M. Gastaldi, T. Pastore, P. Pedeferri, E. Redaelli, *Electrochim. Acta* **2009**, *54*, 1452.
[24] M. Herbrand, V. Adam, M. Classen, D. Kueres, J. Hegger, *Materials* **2017**, *10*.
[25] T. Büttner, *Bautechnik* **2020**, *97*, 48–56.

How to cite this article: Driessen-Ohlenforst C. SMART-DECK: Multifunctional carbon-reinforced concrete interlayer for bridges. *Materials and Corrosion*. 2020;1–11.
https://doi.org/10.1002/maco.202011540